

Effects of Al (2.3-3.3) % and Mo (0.44-1.44) % additives on the electrical conductivity of UNS N04400

Augustine Anyiam Oputa ^{1,*}, Kennedy Chinedu Owuama ¹, Elvis Emifoniye ¹, Reuben Ishiekwene ², Vincent Chukwuemeka Ezechukwu ¹ and P. N. Atanmo ¹

¹ Department of Mechanical Engineering, Chukwuemeka Odumegwu Ojukwu University Uli Campus, Anambra State, Nigeria.

² Department of Electrical/Electronic Engineering, Delta State Polytechnic Ovwashi Uku, Delta State, Nigeria.

World Journal of Advanced Engineering Technology and Sciences, 2025, 16(02), 295-304

Publication history: Received on 12 July 2025; revised on 18 August 2025; accepted on 21 August 2025

Article DOI: <https://doi.org/10.30574/wjaets.2025.16.2.1291>

Abstract

This research investigates the electrical conductivities of aluminium and molybdenum in UNS N04400. Solute mix (Al and Mo) in the solvent and optimization was determined using a design computer software. Research specimens' production was accomplishable with sand casting technique. Cast specimens were machined to ASTM and ISO standards, heat to 950 °C, soaked for one hour and cooled in the furnace. Test samples were loaded into the LSR machine. Specimens test analysis results at (-200, 20 and 900) °C indicate electrical conductivity (1822286.912-1859599.926, 1629687.482-1663056.844 and 1442097.556-1471625.84) S/m and electrical resistivity (0.549-0.538, 0.614-0.601 and 0.693-0.680) $\mu\Omega$ m. Optimization results at 20 °C indicate (1661972.842) S/m and (0.601) $\mu\Omega$ m. Electrical conductivity and resistivity vs temperature graphs were plotted. Comparison of research alloy results at (-200, 20 and 900) °C with that of the solvent and UNS N05500 indicate (49, 17.6, 0.7) % decrease and (2.2, 2.3, 2.2)% increase in electrical conductivities. Solute high solubility, occupation of solvent vacancies, refined lattice grain, increased grain boundaries with formation of largescale precipitates of different sizes. Molybdenum comparative higher numbers of valance electrons provides research samples comparative higher electrical conductivity over UNS N05500. However, temperature increase delocalize and excite delocalized electrons and phonons to higher velocities resulting to electrons and phonons collision and scattering. This impede onward electric current transfer and increase electrical resistivity. In elevated temperature environments, where electrical conductivity and strengths are a priority over strength to weight ratio, UNS N04400 strengthened with Al and Mo is a preference over UNS N04400 and UNS N05500.

Keywords: UNS N04400; UNS N05500; Electrons; Molybdenum; Electrical Conductivity; Temperature

1. Introduction

UNS N04400 is a Nickel copper alloy with excellent corrosion and oxidation resistance typically in seawater, chlorine solutions, acidic and alkaline media and in majority of oxidizing and reducing environments, which involve gases [1- 4]. It has a compressive and tensile strengths, elastic modulus and Poisson ratio of (759, 620) MPa, 179 GPa and 0.32. For strengths improvement, UNS N04400 is alloyed with Al and Ti with heating under controlled conditions to precipitate the submicroscopic particles Ni₃ (Al, Ti) throughout the matrix [2, 6-9]. This resulted in the creation of UNS N05500. Compression and tensile strengths, elastic modulus and Poisson ratio of UNS N05500 is (928, 758) MPa, 179 GPa and 0.32 [5-6, 11-13]. To retain the excellent corrosion and oxidation resistance of UNS N04400 at higher strengths and temperature, it was alloyed with (Al and Mo). UNS N04400 strengthened with (Al and Mo) has a compressive and tensile strengths of (967, 787.4) MPa, an elastic modulus of (183.4) GPa and Poisson ratio of 0.324 [3]. However, despite these properties improvement, the electrical conductivity and resistivity of the research alloy until date remain unknown.

* Corresponding author: Oputa Anyiam Augustine.

Nickel-copper alloys notably maintain outstanding strength, ductility and toughness over broad temperature ranges starting from absolute (0–120) °C [2]. Essentially, this stems from the austenitic matrix of its face centered cubic (FCC) lattice structure [2-3, 8-9]. The FCC lattice structure promotes development of complex twin/dislocation substructure. In addition, it favours outstanding solubility of alloying elements in the solid solution [2, 10-11]. High solubility of alloying elements in the alloy creates large-scale distribution of precipitates in numerous sizes with solubility decrease resulting from temperature drop. UNS N04400 family is formed with major copper additions of (28–34) % by weight. This provides strengthening of the solid solution, improved resistance to corrosion typically in seawater, chlorine solutions, acidic and alkaline media, and numerous oxidizing and reducing environments involving gases. Nickel-copper alloys have outstanding properties that allow their applications for manufacture of numerous machine components such as features and fasteners, heat exchangers, propeller shafts, turbine blades, valves, evaporators, diffusers in steam jet ejectors, assemblies used in chemical, petrochemicals, nuclear and marine plants or facilities [1, 11, 9, 5, and 13]. In addition, they find applications in elevated temperature environments such as in gas turbines, missiles and aerospace systems [2, 11]. As properties differ from one material to the other, so is their applications and uses. This provides some materials choice and or preference to others in engineering/technology applications. One of the areas of interests in metallurgy and materials engineering is materials ability to conduct or resist flow of electric current. Effects of electricity on materials characteristics by description is electrical properties, which describe materials ability/inability to conduct electrical current. [23], variation of materials electrical properties categorize them into good and poor conductors and insulators. These characteristics make them foundation components in electrical/electronic and computer engineering [24]. From the basic wire applications to intricate circuits, electrical properties remain the stronghold of electrical infrastructure and electronic systems. The choice of electrical wires made essentially from metals (copper and or aluminum) is dependent on their outstanding conductivity that enables least losses in energy as heat during transmission. In similar concern, materials with least conductivity find applications in resistors because of their ability to resist current flow thus control flow of electric current. More so, developments in superconductivity; a situation in which some materials exhibit zero resistance to electricity at low temperatures close to 0k (-273 °C) is essentially of enormous importance in revolutionizing of systems; electrical power generation, quantum computing and resonance imaging machinery (MRI). Consequently, design of components (capacitors, conductors, inductors, resistors, amongst others) require excellent understanding of materials electrical properties. Excellent superconductivity results in magnetic levitation, which allows transportation vehicles (trains) to float on magnets with copious superconductivity. Electric generators produced with wires having superconductivity are greatly comparatively better than the ones made from conventional generators having wound copper wire. Use of superconducting wires in electrical power generation and transmission provides for power storage with enhancement in power stability. Studies in physics reveal five principal different types of conductivities; ionic, hydraulic, acoustic, thermal and electrical conductivity. Fundamental electrical properties of engineering materials (solids) are conductivity, resistivity (resistance), superconductivity, magnetism (permittivity, dielectric strength and permeability). These properties are vital in material selection for numerous applications and environments. Primary concerns of majority of design and production engineers is electrical and thermal conductivities [23]. Notably, one of the fundamental characteristics of metals and alloys is electrical and thermal conductivity. Both are comparatively better heat and electricity conductors than nonmetals. Nevertheless, threshold of conductivity within metals and alloys differ considerably because of their microscopic characteristics. Metals and alloys are the center of concern for matters involving advanced applications [2528].

One of the major sources of electrical power generation is conversion of thermal energy into electrical power. Thus, there is increasing demand for thermoelectric materials with elevated temperature application and optimised efficiency [14]. Thermoelectricity is the direct conversion of temperature differences into electric voltage and vice versa using a thermocouple [15-19]. Thermoelectric devices generate a voltage whenever temperature difference occurs on each side of a thermocouple. At the atomic level, temperature difference compel charge carriers in materials to drift away from high temperature regions to lower temperature areas [20]. It is possible to use this effect for generation of electricity, measure and or alter the temperature of a body. Thermoelectric materials are useable as temperature controllers because polarity of applied voltage determine the direction of heating and cooling. [21], thermoelectricity provides description for the reciprocal interaction of temperature with electricity and the conversion of both into each other. [17], thermoelectric effects comprise of three different identified effects; Seebeck effect, Peltier effect and Thomson effect. These three effects usually appear together [20]. Outstanding knowledge and precise understanding of electrical and thermal attributes of materials is a basic requirement for the development of thermoelectric materials with excellent electrical conductivities, enormous Seebeck coefficients and low thermal conductivities. In contemporary times, thermoelectricity increasingly find applications in modern systems, machines and appliances such as in beverage coolers, portable refrigerators, electronic assemblies, metallic sorting software, amongst others. Advantages of thermoelectric generators include long service intervals, durability, outstanding reliability and low maintenance requirements [21]. Emphasis on the role and importance of electricity is inexhaustible in contemporary era. From industrial machinery that apply in manufacture, refining, conversion, recycling, storage, mineral prospection, to those that apply in sports, comedy, music, concerts, home and office appliances, electrical conductivity and resistance remains

a core and prime driver. Understanding material properties is therefore, vital not for only their applications but also for the safety and performance guarantee in systems/machinery where their application is inevitable. Besides, it provides knowledge on how engineers could satisfy their quest in the tailor of materials for different applications, environment(s) and how best to protect materials for longevity in service. This is because no one material can satisfy all properties and application requirement(s) and resist all failure modes in all environment thus materials lifespan whether theoretical or otherwise is nonfinite [22]. Outstanding knowledge of where various and available engineering materials are in the spectrum provides guides to engineers, technologist and manufactures on choice of materials for respective products [23]. The best-engineered materials are prone to failure given sufficiently harsh application environment or if they are poor or wrong choice(s) for specific application(s). Consequently, engineers remain poised to design and develop materials through experimental researches to serve commercial and industrial purposes for the manufacture of devices/systems and components that will operate at maximum efficiency with safety and durability guarantees that ensure components are not either replaced or overhauled in a non-cost effective manner. This research by default investigates the electrical conductivity of UNS N04400 strengthened with (Al and Mo). It involved a design of experiment, which determined solute mix and optimization in the solvent (UNS N04400) that generates maximum electrical conductivity. Test specimens produced by sand casting technique were heat to 950 °C, held for one hour and cooled in the furnace.

2. Materials and methods

Wooden patterns, saw, bail out furnace, moulding box, pattern, synthetic moulding sand, wood turning lathe, emery paper, sand milling machine, scooper, shank, blower, books, design expert software, LSR machine. Solute mix and optimization in the solvent is determined with a computer software for experimental design. Research samples produced by sand casting technique were machined to ASTM and ISO standards, heat to 950 °C, soaked for one hour and cooled in the furnace. Specimens were placed into the sample robot (sample holder) and the sample robot is placed into LSR furnace. The procedures for operation of the LSR machine then followed in sequence.

Table 1. Percentage composition of the research alloy.

S/N	Element	% Composition by weight	Remark
1	Nickel	63	Constant
2	Cobalt	5	Constant
3	Carbon	0.25	Constant
4	Manganese	1.5	Constant
5	Iron	2.0	Constant
6	Sulphur	0.01	Constant
7	Silicon	0.5	Constant
8	Copper	29	Constant
9	Aluminum	2.30 – 3.30	Variable
10	Molybdenum	0.44 – 1.44	Variable

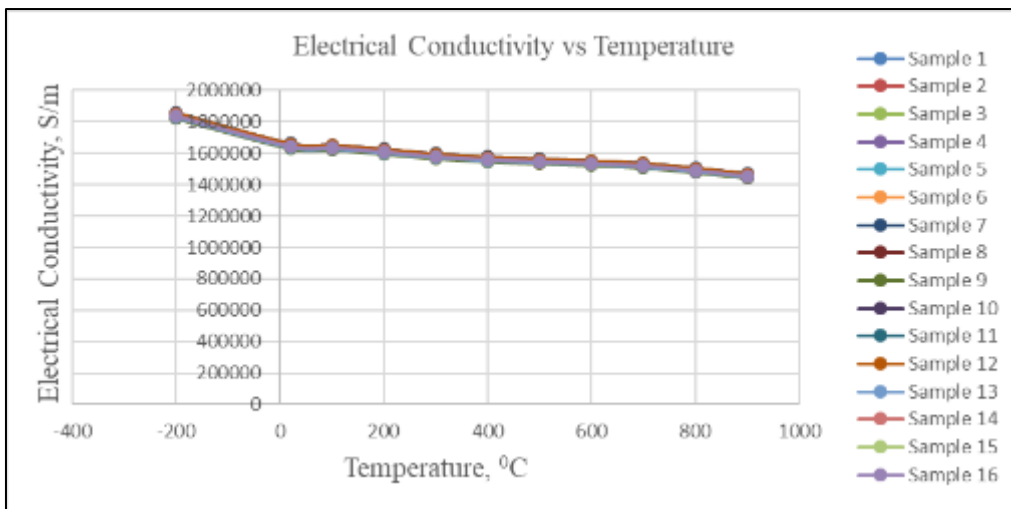
3. Results

Table 2 Electrical conductivity and corresponding temperature effect

Run	Electrical Conductivity; Siemens/meter (S/m)				
	-200 °C	20 °C	100 °C	200 °C	300 °C
1	1839646.725	1645212.518	1637226.05	1611155.571	1580946.404
2	1832184.122	1638538.646	1630584.575	1604619.852	1574533.23
3	1832263.511	1638609.644	1630655.228	1604689.381	1574601.455

4	1854651.32	1658631.262	1650579.654	1624296.538	1593840.978
5	1849623.325	1654134.681	1646104.901	1619893.039	1589520.045
6	1837212.118	1643035.227	1635059.328	1609023.351	1578854.163
7	1859599.926	1663056.844	1654983.753	1628630.508	1598093.686
8	1827235.517	1634113.064	1626180.476	1600285.883	1570280.522
9	1822286.912	1629687.482	1621776.378	1595951.913	1566027.815
10	1837212.118	1643035.227	1635059.328	1609023.351	1578854.163
11	1837212.118	1643035.227	1635059.328	1609023.351	1578854.163
12	1854651.32	1658631.262	1650579.654	1624296.538	1593840.978
13	1829749.514	1636361.354	1628417.852	1602487.632	1572440.989
14	1842240.111	1647531.807	1639534.08	1613426.849	1583175.096
15	1842240.111	1647531.807	1639534.08	1613426.849	1583175.096
16	1837212.118	1643035.227	1635059.328	1609023.351	1578854.163

Run	Electrical Conductivity; Siemens/meter (S/m)					
	400	500	600	700	800	900
1	1561428.547	1549472.739	1537698.63	1521512.329	1492338.788	1455835.537
2	1555094.548	1543187.239	1531460.893	1515340.252	1486285.055	1449929.881
3	1555161.931	1562110.607	1531527.251	1515405.911	1486349.456	1456485.748
4	1574163.929	1562110.607	1550240.465	1533922.145	1504510.658	1467709.678
5	1569869.341	1557875.695	1546037.734	1529763.652	1500431.901	1463730.689
6	1559362.137	1547422.151	1535663.624	1519498.744	1490363.812	1453908.87
7	1578364.134	1566278.651	1554376.838	1538014.976	1508525.013	1471625.84
8	1550894.343	1539019.195	1527324.52	1511247.42	1482270.7	1446013.718
9	1546694.138	1534851.151	1523188.148	1507154.589	1478256.344	1442097.556
10	1559362.137	1547422.151	1535663.624	1519498.744	1490363.812	1453908.87
11	1559362.137	1547422.151	1535663.624	1519498.744	1490363.812	1453908.87
12	1574163.929	1562110.607	1550240.465	1533922.145	1504510.658	1467709.678
13	1553028.137	1541136.65	1529425.886	1513326.666	1484310.078	1448003.212
14	1563629.724	1551657.062	1539866.355	1523657.235	1494442.568	1457887.858
15	1563629.724	1551657.062	1539866.355	1523657.235	1494442.568	1457887.858
16	1559362.137	1547422.151	1535663.624	1519498.744	1490363.812	1453908.87

**Figure 1** Electrical conductivity responses to temperature changes**Table 3** Electrical resistivity and corresponding temperature effect

Run	Electrical Resistivity ($\mu\Omega \cdot m$)				
	-200 °C	20 °C	100 °C	200 °C	300 °C
1	0.544	0.608	0.611	0.621	0.633
2	0.546	0.610	0.613	0.623	0.635
3	0.546	0.610	0.613	0.623	0.635
4	0.539	0.603	0.606	0.616	0.627
5	0.541	0.605	0.608	0.617	0.629
6	0.544	0.609	0.612	0.622	0.633
7	0.538	0.601	0.604	0.614	0.626
8	0.547	0.612	0.615	0.625	0.637
9	0.549	0.614	0.617	0.627	0.639
10	0.544	0.609	0.612	0.622	0.633
11	0.544	0.609	0.612	0.622	0.633
12	0.539	0.603	0.606	0.616	0.627
13	0.547	0.611	0.614	0.624	0.636
14	0.543	0.607	0.610	0.620	0.632
15	0.543	0.607	0.610	0.620	0.632
16	0.544	0.609	0.612	0.622	0.633

Run	Electrical Resistivity ($\mu\Omega \cdot m$)					
	400 °C	500 °C	600 °C	700 °C	800 °C	900 °C
1	0.640	0.644	0.650	0.657	0.670	0.687
2	0.643	0.648	0.653	0.660	0.673	0.690
3	0.643	0.648	0.653	0.660	0.673	0.687

4	0.635	0.640	0.645	0.652	0.665	0.681
5	0.637	0.642	0.647	0.654	0.667	0.683
6	0.641	0.646	0.651	0.658	0.671	0.688
7	0.634	0.639	0.643	0.650	0.663	0.680
8	0.645	0.650	0.655	0.662	0.675	0.692
9	0.647	0.652	0.657	0.664	0.677	0.693
10	0.641	0.646	0.651	0.658	0.671	0.688
11	0.641	0.646	0.651	0.658	0.671	0.688
12	0.635	0.640	0.645	0.652	0.665	0.681
13	0.644	0.649	0.654	0.661	0.674	0.691
14	0.640	0.645	0.649	0.656	0.669	0.686
15	0.640	0.645	0.649	0.656	0.669	0.686
16	0.641	0.646	0.651	0.658	0.671	0.688

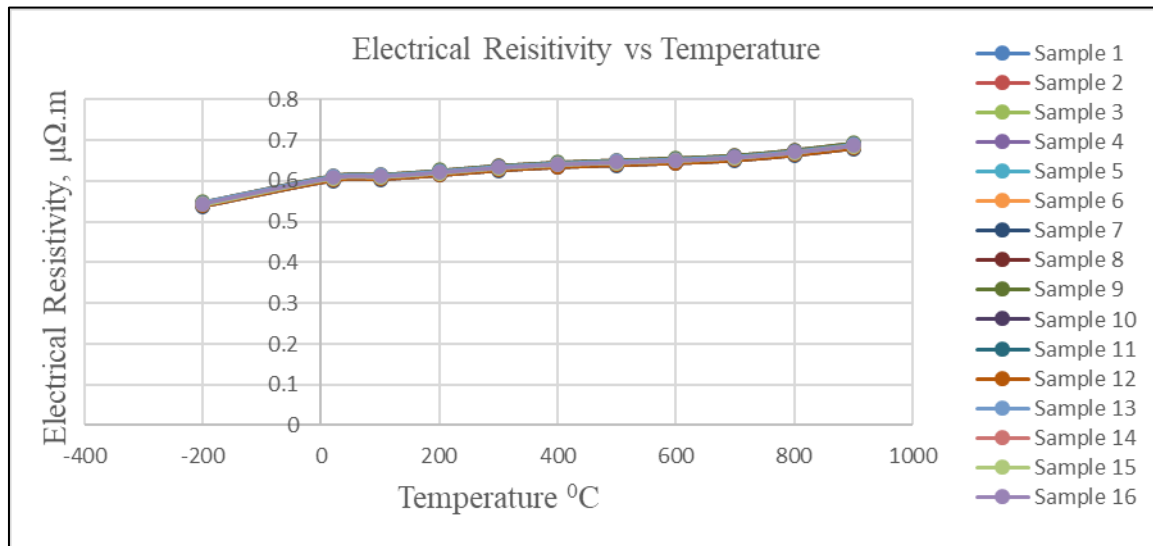


Figure 2 Electrical resistivity response to temperature changes

4. Result Optimization

Table 4 Electrical conductivity (goal: maximize)

Number	Al	Mo	Electrical Conductivity	Desirability	
1	3.300	1.342	1661972.842	0.809	Selected
2	3.300	1.346	1662021.118	0.809	
3	3.300	1.336	1661905.281	0.809	
4	3.300	1.274	1661216.185	0.799	
5	3.300	1.270	1661175.069	0.798	
6	3.300	1.241	1660852.900	0.790	

5. Comparison of Research Sample Electrical Conductivity and Resistivity with that of UNS N04400 and UNS N05500

Table 5 Room temperature comparison of research alloy electrical conductivity with that of UNS N04400 and UNS N05500

Run	Property	Unit	Research Alloy	UNS N05500	UNS N04400
	Electrical Conductivity	S/m	1663056.842	1626016.26	1956947.162

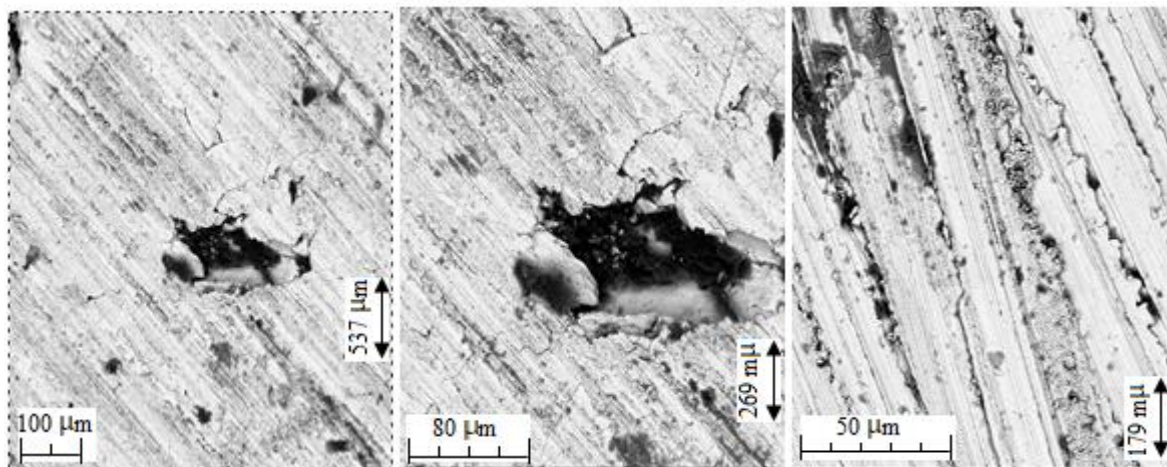


Figure 3. SEM image of research samples show columnar, equiaxed grains structure with block particle Mo-C primary carbides. Magnification (a) 500x (b) 1000x (c) 1500x

6. Discussion

Research specimens' crystallography reveal solute high solubility in the solvent. This reflects solute adequate dissolution and filling of solvent interstitial sites with formation of fine grains, multiple grain boundaries, dislocation restriction and presence of largescale distribution of block particles (Mo-C) primary carbide of numerous sizes. These microstructural features no doubt asserts strengths improvement in the research alloy as reported in previous experiments by [3]. Grain size refinement and increase in grain boundaries are notable to impede plastic deformation with notable strengths improvement. Svea, et al had earlier studied the strengthening effect produced by grain size reduction from the blockage of dislocations by grain boundaries. A fine-grained material is stronger than one that is coarse grained, since the former has a greater total grain boundary area to obstruct dislocation motion.

Degree of grain refinement created by alloying is a reference to the solubility of the solute in the solvent. Solute high solubility in the solvent is because of the distance between the former and later in the electrochemical series (periodic table) of elements, and the comparatively smaller size of the solute (4.74) % in the solvent (95.26) %. Consequently, the solute dissolve adequately in the solvent filling vacancies in the solvent crystal lattice to form a single face phase interstitial solid solution. This provides barrier to dislocation motion, which improved the research alloy Peiers-Nabarro stress (stress required to move dislocations) and subsequently, improve the research alloy resistance to deformation. This is possible since restriction of dislocation motion is one method of strengthening metals. Alloy strengthening is achievable by either generating internal stress that oppose dislocation motion, or by placing particles in their path, which require them to cut or loop the particles. Test specimens SEM analysis reveal single-phase interstitial solid solution with a face-centered cubic crystalline structure that contain block particles (Mo-C) primary carbide. These carbides are well ordered with uniform and visible homogeneous distributions in intergranular and intragranular locations. Lattice grains exhibit proper order with visible twins (annealing twins) and stacking faults, fig. 3. The block particles (Mo-C) primary carbides suggests presence of secondary phase however, it is not. This is because the solute weight percentage is greatly less than the requirement to exceed the solubility limit of the solvent. Besides, unlike UNS N05500 research samples were not aged. Research samples lattice grains is characterized with columnar and equiaxed particle structure (grains), which evidently reveal $<100>/\text{CD}$ and $<111>\text{CD}/\text{CD}$ orientation fibers, fig. 3. The $<110>/\text{CD}$ fiber texture include the $\{001\}$ $<100>$ cube texture and $\{110\}$ $\{001\}$ Goss texture. The $<111>/\text{CD}$

include $\{112\} <111>$ copper texture and $\{110\} <111>$ texture, fig. 3. Dislocation arrangements in the crystalline is planar in majority of the grains regions, with dislocation twins visible in the absence of any marked tendency for dislocation distribution along a properly defined planar array or pairing. Technically, this relates high stacking fault energy in the research alloy with absence of short-range order. It is worth mentioning that nickel has high stacking fault energy, which could decrease by alloying as in Ni-Cr base alloys. Besides, presence of copper in substantive quantity in UNS N04400 could reduce stacking fault energy. However, following the presence of very small quantities of alloying elements in UNS N04400, nickel stacking fault energy remain not affected or reduced with copper addition. Thus stacking fault change in Ni-Cu matrix is most likely small. It is suffix to recall Raynor, and Silcock in their studies on some γ^1 hardened alloys observed tangled dislocation arrangements in solution treated, and deformed condition. Both concluded such arrangements is due to the stacking fault energy of UNS N04400 metals.

Alloy strengthening effect relies on the nature of interactions of the dislocation with the solute atoms. Most often, two general interactions exist which are considered. One is of a chemical nature in which the difference in chemical bonding between solute atoms and solvent atoms reflects in the difference in their elastic shear moduli. This effects a change in the dislocation-atom interaction. In other words, the foremost reason grain boundaries act as barriers to dislocation motion during plastic deformation is because grains are of different crystallographic orientations. Therefore, as dislocation pass from one grain to another its direction of motion alters. Besides, as the mis-orientation between the grains increases, the process is restricted the more, fig. 3a, b and c. The other interaction is an elastic nature in which if the size of the solute atoms differ from those of the substance (solvent) atoms, then a misfit strain field forms around the solute atom that interacts with the strain field of the dislocations. In other words, atomic disorder inside a grain boundary region triggers discontinuity of slip planes from one grain into the other. Therefore, the boundaries separating two different phases also constitute barriers to dislocations. This behavior apply for strengthening metallic materials with complex multi-phase(s). The crystallography reorientation confirms the research alloy possess great electrostatic force (metallic bond). This is evident in the research alloy greater compressive and tensile strengths and elastic modulus (967, 787.4) MPa, (183.3) GPa in comparison to the solvent (759, 620) MPa, (179) GPa and UNS N05500 (928, 758) MPa, (179) GPa as reported in previous research by [3]. Obviously, these properties improvement stem from molybdenum greater number of valence electrons, ionization energy and electron affinity, which characterize grain refinement, increase in grain boundaries and restriction of dislocation motion. However, these microstructural changes accounts for the solvent greater electrical conductivity (1956947.162) S/m and lower resistivity in comparison to the research alloy (1663056.842) S/m and UNS N05500 (1626016.26) S/m. The reason for this is that electrical resistivity is dependent on defects or imperfections, mechanical stress and temperature. Defects (grain boundaries, dislocations, interstitial atoms, vacancies) in material crystal lattice lowers conductivity because defects act as barriers to energy flow between the grain boundaries and particles thus impede electrical energy flow through materials crystal lattice. This point to vital attributes of microstructures because grain boundaries are frequently points of internal weakness on which failure by fracture or corrosion will grow or spread through materials interfacial network. Concentration of imperfections is dependent on composition, magnitude of cold work and temperature on materials (metal and or alloy). This provides reason annealed materials (metals and alloys) with large crystals have higher conductivity and lower resistivity. While work hardened materials, have lower conductivity and higher resistivity. Experimental details reveal absolute resistivity of materials consist of the overall contributions from impurities, plastic deformations and thermal vibrations that scatter the mechanisms, acts independent of one another. However, electrical properties like mechanical properties of solids typically metallic materials is greatly dependent on details of microstructure and molecular interactions. Propagation of these properties occur by the transfer of respective energies and or signals through materials by a combination of diffusion of valence electrons and lattice vibrations (phonons). Molybdenum holds six valence electrons unlike titanium with four. This differential increase provide research specimens leverage and greater electrical conductivity and lower electrical resistivity [(1663056.842) S/m and (0.601) $\mu\Omega\cdot m$] in comparison to UNS N05500 [(1626016.26) S/m and (0.615) $\mu\Omega\cdot m$]. This is because electricity is simply a swamp of moving electrons (electron flow), while potential difference is the force, which propel current flow. Electric current application, excite delocalized electrons and transfer electrical charge at tremendous speed through the alloy. Consequently, with potential difference, delocalized electrons travel at tremendous speeds and transmits comparatively greater electric charge through the research specimens' than is obtained in UNS N05500. Increase in molybdenum percentage corresponds to increase in research samples electrical conductivity and vice versa, table 2. Optimization reveals solute mix of Al 3.3% and Mo 1.44% maintains maximum electrical conductivity, table 4. Potential difference application across the research alloy, results in travel of localized electrons in the alloy crystal lattice toward the positive electrode. Simultaneously free valence electrons, which travel from the negative electrode, replace electrons, which travel to the positive electrode. Consequently, flow of electrons in the alloy is maintained from the negative electrode. Lattice vibration (phonons) also partake in electrical conductivity however, electrons transfer dominates.

Temperature effect on research specimens, tables 2, 3 and figs. 1 and 2 reflects decrease and increase in electrical conductivity and resistivity. This is because temperature increase provide energy to localized electrons and phonons

enabling both (especially) localized electrons to travel at relatively greater speeds. At high speeds, delocalized electrons and phonons collide and scatter more frequently. High velocity collision and scattering of electrons and phonons weaken forward electron flow and increase electrical resistivity with corresponding decrease in electrical conductivity. In addition, temperature increase volume while mass remains unchanged, lattice grains coalesce, grain boundaries and dislocations restrictions collapse. These crystallographic changes enhance phonons collision and scatter and distort research samples lattice arrangements, reduce Peiress-Naborro stress resulting to decrease in electrical conductivity. Graph of electrical conductivity and resistivity with corresponding temperature effects, figs. 1 and 2 slopes downwards and upwards reflecting decrease and increase in electrical conductivity and resistivity.

7. Conclusion

Solute (Al and Mo) high solubility and occupation of the solvent interstitial sites (vacancies) refined grain sizes, increased grain boundaries, reduced dislocation motion and improved the Peiress-Naborro stress of the research alloy. These crystallographic changes resulted in UNS N04400 greater electrical conductivity in comparison to the research alloy and UNS N05500.

Molybdenum comparative greater number of valence electrons increased availability of localized and delocalized electrons and greater electrical conductivity of the research alloy in comparison to UNS N05500.

Temperature increase excite localized electrons, coalesce grain sizes, collapse grain boundaries, increase dislocation motion thereby mobilize phonons. These crystallography interference cause electrons and lattice particles to travel at higher speeds.

At high velocity travels, delocalized electrons and phonons collide and scatter more frequently impeding onward transfer of electrical signals. Consequently, temperature increase reduced electrical conductivity and increased electrical resistivity in the research specimens.

Recommendations

In applications where electrical conductivity and strengths are basic requirements, and temperature increase above room temperature is inevitable, UNS N04400 strengthened with Al and Mo is a preference over UNS N04400 and UNS N05500.

Compliance with ethical standards

Disclosure of conflict of interest

No conflict of interest to be disclosed.

References

- [1] Mateusz Kukliński, Aneta Bartkowska & Damian Przestacki (2018). Microstructure and Selected Properties of Monel 400 Alloy after Laser Heat Treatment and Laser Boriding using Diode Laser. *The International Journal of Advanced Manufacturing Technology*, 98:3005–3017. <https://doi.org/10.1007/s00170-018-2343-9>. Springer.
- [2] A. G. Kostryzhev, O. O. Marenich, Z. Pan, H. Li & S. van Duin (2023). Strengthening Mechanisms in Monel K500 alloyed with Al and Ti. *J Mater Sci of Metals and Corrosion* 58:4150–4164.
- [3] Augustine Anyiam Oputa, Kennedy Chinedu Owuama, Elvis Emifoniye, Vincent Chukwuemeka Ezechukwu & P.N. Atanmo (2025). Strengthening Potentials of Aluminium (2.3-3.3) % and Molybdenum (0.44-1.44) % Additives on the Compressive and Tensile Strengths of Monel 400. *World Journal of Advanced Research and Reviews*, 27(02), 561-571.
- [4] Smiths (2023). Monel K500. Product Datasheet. Nickel-Copper Alloy. Smiths Metal Centers. www.smithmetal.com
- [5] Ulbrich (2014). Monel 400, UNS 04400. Strip, Coil, Foil, Wire, AMS, 4544, QQ-N 2810D, ASTM B127. Ulbrich Stainless Steels and Special Metals Inc. ulbrich.com
- [6] Ulbrich (2014). Monel k500 (Alloy k500), UNS N05500 Shaped Flat, Square, Round, Fine Wire, Plated and Unplated ASTM B865, AMS 4676, QQ-N 286. Ulbrich Stainless Steels and Special Metals Inc. ulbrich.com

- [7] Special Metals (2000). High-Performance Alloys for Resistance to Aqueous Corrosion. Special Metals Corporation, SMC-026. Available at specialmetals.com
- [8] Special Metals (2002). Monel Alloy 400. Special Metals Corporation, SMC-053. Available at specialmetals.com
- [9] Special Metals (2004). Monel Alloy K-500. Special Metals Corporation, SMC-062. Available at specialmetals.com
- [10] D. Franzen, B. Pustal, and A. Bührig-Polaczek (2020). Mechanical Properties and Impact Toughness of Molybdenum Alloyed Ductile iron. International Journal of Metalcasting. <https://doi.org/10.1007/s40962-020-00533-z>. Springer.
- [11] Olexandra Marenych, Andrii Kostryzhev, Chen Shen, Zengxi Pan, Huijun Li and Stephen van Duin (2019). Precipitation Strengthening in Ni-Cu Alloys Fabricated Using Wire Arc Additive Manufacturing Technology. *Metals* 9, 105, pp 1-14, doi: 10.3390/met9010105. MDPI.
- [12] M. Zielińska, M. Yavorska, M. Poręba, J. Sieniawski (2010). Thermal Properties of Cast Nickel Based Superalloys. *Archives of Materials Science and Engineering*, vol. 44 (1), pp 35-38. World Academy of Materials and Manufacturing Engineering
- [13] VDM Metals International GmbH (2016). VDM Alloy Nicoros. VDM Metals. International GmbH. Available at www.vdm-metals.com
- [14] Netzscht (2022). Thermal Properties of Metals and Alloys. NETZSCH-Gerätebau GmbH Wittelsbacherstraße 42 95100 Selb Germany.
- [15] Ajai Rai (2022). Introduction to Sustainable Energy Technologies (SEE605A) Experiment on Basic electronics measurement – 2 (SEEBECK AND PELTIER EFFECT). Department of Sustainable Energy Engineering, Indian Institute of Technology Kanpur.
- [16] Ashish Kumar1, Ashutosh Patel, Saurabh Singh, K. Asokan, D. Kanjilal (2019). Apparatus for Seebeck Coefficient Measurement of Wire, Thin Film and Bulk Materials in the Wide Temperature Range (80 – 650) K.
- [17] Christophe Goupil, Henni Ouerdane, Knud Zabrocki, Wolfgang Seifert, Nicki F. Hinsche, & Eckhard Müller (2016). Continuum Theory and Modelling of Thermoelectric Elements, First Edition. Wiley-VCH Verlag GmbH & Co. KGaA.
- [18] Eric Pop (2017). Thermoelectrics 101. EE 323: Energy in Electronics, pp 1-56. Available at <http://poplab.stanford.edu>
- [19] Novela Auparay (2013). Room Temperature Seebeck Coefficient Measurement of Metals and Semiconductors. Project for Award of degree of Bachelor Science in Physics. Oregon State University.
- [20] Uri Lachish, (2020). Thermoelectric Effect Peltier Seebeck and Thomson. Researchgate Journal pp 1-12 DOI: 10.13140/RG.2.2.25436.13444.
- [21] Pobierz, Naszą & Wizytówkę (2023). Thermoelectric Materials Instrumentation for the Characterization of Materials and Modules. [Www.Haas.com.pl](http://www.haas.com.pl)
- [22] Catherine Houska (2000). Metals for corrosion resistance: Part II pp 8-14. The Construction Specifications Institute, 99 Canal Center Plaza, Suite 300, Alexandria, VA 22314.
- [23] Jason Bergman (2024). Metal Properties, Physical Properties, Conductivity. Eagle Group Manufacturing 231-788-2351 5142 Evanston Avenue Muskegon, MI 49442
- [24] Hany S. Abdo, Asiful H. Seikh, Jabair Ali Mohammed & Mahmoud S. Soliman (2021). Alloying Elements Effects on Electrical Conductivity and Mechanical Properties of Newly Fabricated Al Based Alloys Produced by Conventional Casting Process. *Materials* 14, 3971, <https://doi.org/10.3390/ma14143971>. MDPI.
- [25] Gerhard Huber, Miller B. Djurdjevic & Srecko Manasijevic (2019). Determination of Some Thermo-Physical and Metallurgical properties of Aluminum Alloys using their Known Chemical Composition. *International Journal of heat and Mass Transfer* pp 548-553. Elsevier.
- [26] Enrico Lucon, Kenji Abiko, Marlies Lambrecht & Birgit Rehmer (2015). Tensile Properties of Commercially Pure, High-Purity and Ultra-High-Purity Iron: Results of an International Round Robin. *NIST Technical Note 1879*, National Institute of Standards and Technology U.S. Department of Commerce.
- [27] Fritz Klocke (2009). Manufacturing Processes 2. Springer-Verlag BerlinHeidelberg ISBN 978-3-540-92258-2 e-ISBN 978-3-540-92259-9, DOI 10.1007/978-3-540-92259-9, RWTH edition ISSN 1865-0899, e-ISSN 1865-0902.
- [28] Grigory Dyakonov, Sergey Mironov, Tatyana Yakovleva & Irina Semenova (2020). Thermal Stability and Recrystallization of Titanium Grade 4 with Ultrafine-Grained Structure. *MATEC Web of Conferences* 321, 11060. The 14th World Conference on Titanium. EDP Series. <https://doi.org/10.1051/matecconf/202032111060>.